Surface Tension Manipulation with Visible Light through Sensitized Disequilibration of Photoswitchable Amphiphiles

Julius Gemen,§ Bastian Stövesand,§ Frank Glorius,* Bart Jan Ravoo*

Universität Münster, Organisch-Chemisches Institut, Corrensstraße 36, 48149 Münster, Germany

§These authors contributed equally.

*Correspondence to: glorius@uni-muenster.de; b.j.ravoo@uni-muenster.de

ABSTRACT: The light-induced N=N double bond isomerization of azoarenes lies at the heart of numerous applications ranging from catalysis, energy storage, or drug release to optogenetics and photopharmacology. While efficient switching between their *E* and *Z* states has predominantly relied on direct UV light excitation, a recent study by Klajn and co-workers introduced visible light sensitization of *E* azoarenes and subsequent isomerization as a tool coined disequilibration by sensitization under confinement (DESC) to obtain high yields of the out-of-equilibrium *Z* isomer. This host-guest approach is, however, still constrained to small, minimally substituted azoarenes with limited applicability and functionality in advanced multicomponent molecular systems. Herein, we expand the DESC concept to steer the supramolecular assembly of surfactants at the air-water interface. Leveraging our expertise with photoswitchable arylazopyrazole amphiphiles, we induce substantial alterations of the surface tension and surface excess of water through their reversible *E*-*Z* isomerization. After studying the binding of positively and negatively charged surfactants to the host, we find that the extent of surface activity differences upon visible light irradiation for both isomer states is comparable to those observed for direct UV light excitation. The method is demonstrated on large range of concentrations (from μM to mM) and can be equally activated using green or red light, depending on the sensitizer chosen. The straightforward implementation of visible light photoswitch sensitization in a complex molecular network showcases how DESC enables the improvement of existing light-responsive systems and allows for the development of novel applications driven exclusively with visible light.

INTRODUCTION

Derivatives of azobenzene enable the use of light as a non-invasive stimulus to control the properties of matter on various length scales.[1–3] Among many other applications, photoswitches based on the N=N double bond motif hold significant promise in energy storage technologies,[4,5] provide possibilities to steer the target affinity of drug molecules,[6,7] or allow to control catalyst activity.[8–11] Beyond that, azoarenes enable light control for the assembly of nanosized building blocks into one- (e.g., supramolecular polymers),[12–16] two- (e.g., interfaces),[17–19] or three-dimensional (e.g., micro- or nanoparticle assemblies) matter.[20,21]

In all cases, the underlying concept relies on the activation of the *E* azo double bond into its *Z* form,[22] which is associated with significant changes of the molecule's shape and dipole moment. Due to the overlap of both isomers' nπ* bands, activating the photoswitch by specifically irradiating the *E* isomer is commonly limited to UV light (ca. 350 nm) excitation of its ππ* band.[23,24] This requirement of high-energy radiation represents a significant limitation of azobenzene's applicability, especially for its embedment in real-world, for example biological, environments. Existing strategies to circumvent this problem aim to decorate azobenzene's aromatic core with selected substituents that result in spectral separation of *E* and *Z*'s nπ* bands and hence allow to specifically address the thermodynamically stable *E* state using visible light.[25–28] Such molecule designs are connected with significant synthetic effort and, more importantly, change the identity of the photoswitch which affects its function within a given system.

Recently, Klajn and co-workers presented a strategy that allows for the activation of small molecule azoarenes without the necessity of their synthetic modification.[29] By confining the *E* photoswitches with a visible light absorbing photosensitizer as heterodimers within a nanopore[30] (for the molecular components, see Fig. 1A), isomerization with energies corresponding to green, yellow, orange, or red light could be achieved through an energy transfer process.[31–33] Crucially, the *Z* isomer of the applied switches is sterically more demanding and hence does not form analogous heterodimers with the respective sensitizers, preventing *Z*-to-*E* isomerization and accordingly resulting in its accumulation. This strategy, termed disequilibration by sensitization under confinement (DESC), if applicable beyond the proof-of-concept scope of small molecule photoswitches, represents a fundamentally new strategy to control complex molecular systems using light of desired wavelength. However, while the structural flexibility of **H** generally allows for the

confinement of azoarenes with diverse aryl substituents, existing reports are limited to the encapsulation of small-molecule photoswitches without inherent system function.[29,34–37]

Our team has recently investigated photoresponsive surfactants and their impact on the surface tension of water.[38,39] Our studies expanded upon previous reports on charged[40–46] or non-charged[47] amphiphilic azobenzene derivative assemblies at air-water interfaces with significant differences in surface activity for both isomers. In general terms, this concept enables the integration of two different surfactants (*E* and *Z*), each with inherent surface properties, within one molecular design and the reversible switching between both states. We focused on surfactants based on the arylazopyrazole (AAP) moiety,[48] which was initially introduced by Fuchter et al.[49] and exhibits superior photophysical properties over conventional azobenzene derivatives, including higher photostationary states obtainable or more pronounced differences in dipole moment between both isomers. We specifically investigated the UV light induced isomerization of an anionic AAP surfactant and the connected structural organization of both isomer species at the air-water interface. Upon irradiation, significant physicochemical surface property changes are detected and can be connected to an unexpected monolayer-to-bilayer transition. Compared to other existing photoswitchable anionic surfactants, the applied amphiphile demonstrated superior performance in view of the substantial yet reversible surface tension changes ($\Delta\gamma$ = 27 mNm^{-1}).[39]

We envisioned that such systems incorporating charged AAP surfactants (such as positively charged **POS** and negatively charged **NEG**, Fig. 2A) could be controlled using visible light when employing DESC. Specifically, we expected that the green or red light induced *E*-to-*Z* transformation would directly affect the probability of presence of the respective chemical species at the air-water interface and hence modulate the surface tension of water (Fig. 1B). We employ green (**G**) and red (**R**) light absorbing sensitizers in combination with the palladium-based, water soluble coordination cage **H**, whose ability to encapsulate photoswitchable azobenzenes[35], AAPs[36], and azobispyrazoles[29] in the form of homodimers has previously been reported. Subsequent irradiation with green or red light addresses the sensitizer·*E*-surfactant heterodimers and is expected to drive the system away from equilibrium[50–52] while increasing the surface tension; a process, that is reversible by direct excitation of the accumulated *Z* isomer.

RESULTS AND DISCUSSION

Surfactant encapsulation

We initiated the study with the positively charged AAP derivative **POS** (Fig. 2A), which was dissolved in D_2O and titrated with host **H**. Homodimeric binding of photoresponsive AAP-based surfactants bearing two substituents of substantial lengths at opposite sides of the chromophore would result in a pseudorotaxane-type[53] structure with two thread units complexed by a single ring. Despite its positive charge and the resulting Coulombic repulsion with **H**, the significant shifts of **POS**'s proton signals qualitatively confirmed

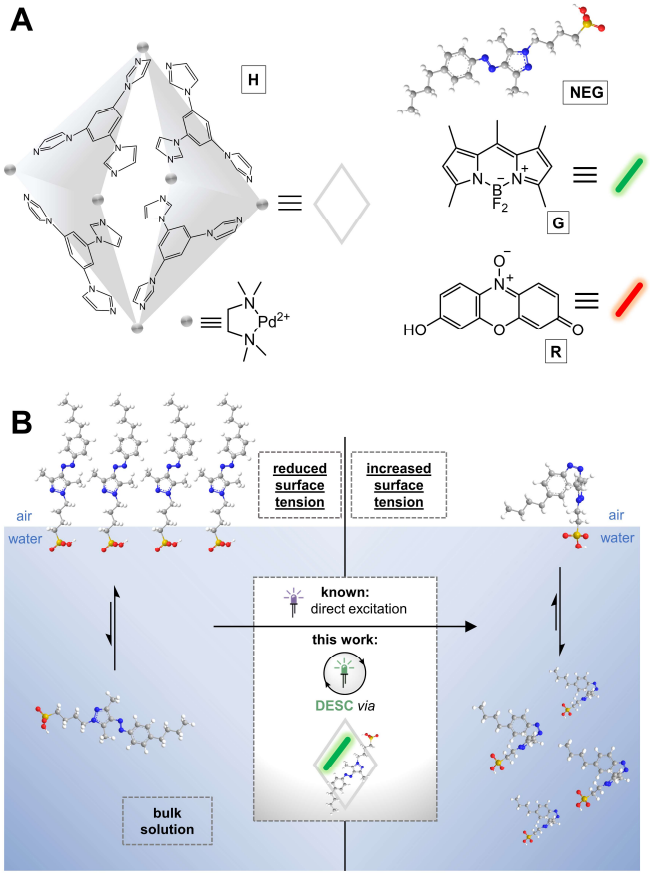

Figure 1. (A) Molecular components of the applied system: host **H** containing six Pd[tmeda]$^{2+}$ nodes and four 1,3,5-tri(1*H*-imidazol-1-yl)benzene ligands, photoswitchable AAP surfactant (here: **NEG**, for molecular structures of **POS** and **NEG**, see Fig. 2A), and photosensitizers **G** and **R**. (B) Scheme: Tuning the surface tension of water by applying light-addressable surfactants.

the formation of the (*E*-**POS**)$_2$⊂**H** complex (Fig. 2B, see Fig. S16 for the stoichiometric binding analysis). Diffusion-ordered spectroscopy revealed identical diffusion coefficients for both species, confirming quantitative association (Fig. S11). Comprehensive structural characterization using various 2D NMR techniques facilitated quantitative peak assignment and provided a detailed understanding of the solution binding mode (Fig. S12–15). We found that signals corresponding to **POS**'s aromatic core and *n*-butyl substituent (red in Fig. 2A+B) were significantly upfield shifted as a result of electron shielding. The benzene protons experienced a shift by $\Delta\delta$ = −1.25 ppm and −0.85 ppm (from 7.34 ppm and 6.82 ppm for **POS** in $CDCl_3$ to 6.09 ppm and 5.97 ppm in (*E*-**POS**)$_2$⊂**H**). The same was found for the para-CH_2-substituent ($\Delta\delta$ = −0.59 ppm). In contrast to that, protons of the trimethylammonium linker at the pyrazole unit experienced a significant deshielding effect (blue in Fig. 2A+B), resulting in a downfield shift. Exemplarily, pyrazole's methylene substituent and the methylene group adjacent to the NMe_3 group were shifted by +0.19 ppm and +0.24 ppm (from 3.97 ppm and 3.49 ppm to 3.97 ppm and 3.25 ppm, respectively). This underscores the binding site of **H** being specifically the aromatic and hydrophobic end of the surfactant in an effort to maximize the distance to the positively

charged head group. We applied isothermal titration calorimetry (ITC) to quantify the binding energy of *E*-**POS** to **H** (K_a = 2.06·10^4 M^{-1}, in a 1:1 binding model, see SI Chapter 5 for details), which, due to its positive charge, was found to be significantly lower than for previously reported guests.[54,55] The binding process is still driven by enthalpy, as the encapsulation of the surfactants into **H**'s cavity is an exothermic process (ΔH = −22.64 kJmol^{-1}) that is connected with a decrease in disorder (ΔS = −4.91 Jmol^{-1}K^{-1}).

Converting *E*-**POS** to *Z*-**POS** by UV light irradiation (365 nm) was not hindered by the presence of **H** (Fig. S17). After isomerization, a downfield shift of signals corresponding to hydrophobic protons (red) and an upfield shift of hydrophilic proton signals (blue) was observed. This aligns with the lower binding energy of the *Z* isomer to **H**, which is a crucial prerequisite for DESC (see below). The process was reversible by irradiation with green light (515 nm).

Analogous binding studies were performed for the negatively charged surfactant **NEG**. While equally forming homodimeric complexes, in-depth analysis of the (*E*-**NEG**)$_2$⊂**H** complex revealed binding of **H** to the hydrophilic (blue) end of the molecule (Fig. S18–21). This is suggested by electron shielding effects observed specifically for **NEG**'s sulfonate linker and follows expected Coulombic attraction. The binding strength of the negatively charged surfactant to **H** was confirmed to be significantly higher (K_a = 5.06·10^6 M^{-1}) than for **POS**. While showing analogous parameter trends, the enthalpic and entropic effects are much more distinct for **NEG**, as the encapsulation process is connected with a highly exothermic reaction (ΔH = −400.38 kJmol^{-1}) combined with a significant decrease in disorder (ΔS = −1225.38 Jmol^{-1}K^{-1}).

Heterodimer formation and green light DESC

To specifically address the amphiphiles' *E* isomers with visible light, we studied their ability to form sensitizer·surfactant heterodimers within **H**. We synthesized homodimer complex (**G**)$_2$⊂**H** bearing the green light absorbing BODIPY derivative **G**. To its aqueous (20 μM) solution, we added aliquots of (*E*-**NEG**)$_2$⊂**H**. As followed by UV-vis spectroscopy, and in analogy to the behavior described previously for the small-molecule **AAP-Me**[29], significant formation of the heterodimer species (*E*-**NEG**·**G**)⊂**H** was apparent based on the decrease of (**G**)$_2$⊂**H**'s characteristic absorption at 480 nm and the simultaneous formation of a new band centered at 509 nm corresponding to the heterodimer complex (Fig. 2C).[56] We found **NEG**'s tendency of heterodimer formation to be similar to **AAP-Me**. In contrast, the heterodimer formation of **POS** with **G** observed on UV-vis spectroscopy was significantly lower, correlating with its low host association at low micromolar concentration (Fig. 2D).

Following the reaction scheme depicted in Fig. 3A, irradiating a solution containing the heterodimer (*E*-**NEG**·**G**)⊂**H** with green light close to its absorption maximum (λ_{exc} = 515 nm) resulted in a fast accumulation of *Z*-**NEG** (Fig. 3B). The observed reaction kinetics were analogous to those of previously reported **AAP-Me** (Fig. S26), indicating an analogous mode of action in place. The isomerization of the surfactant could be reversed by irradiation with blue light (434 nm), with no fatigue observed over ten cycles of green and blue light irradiation (Fig. 3C). Gradually decreasing the

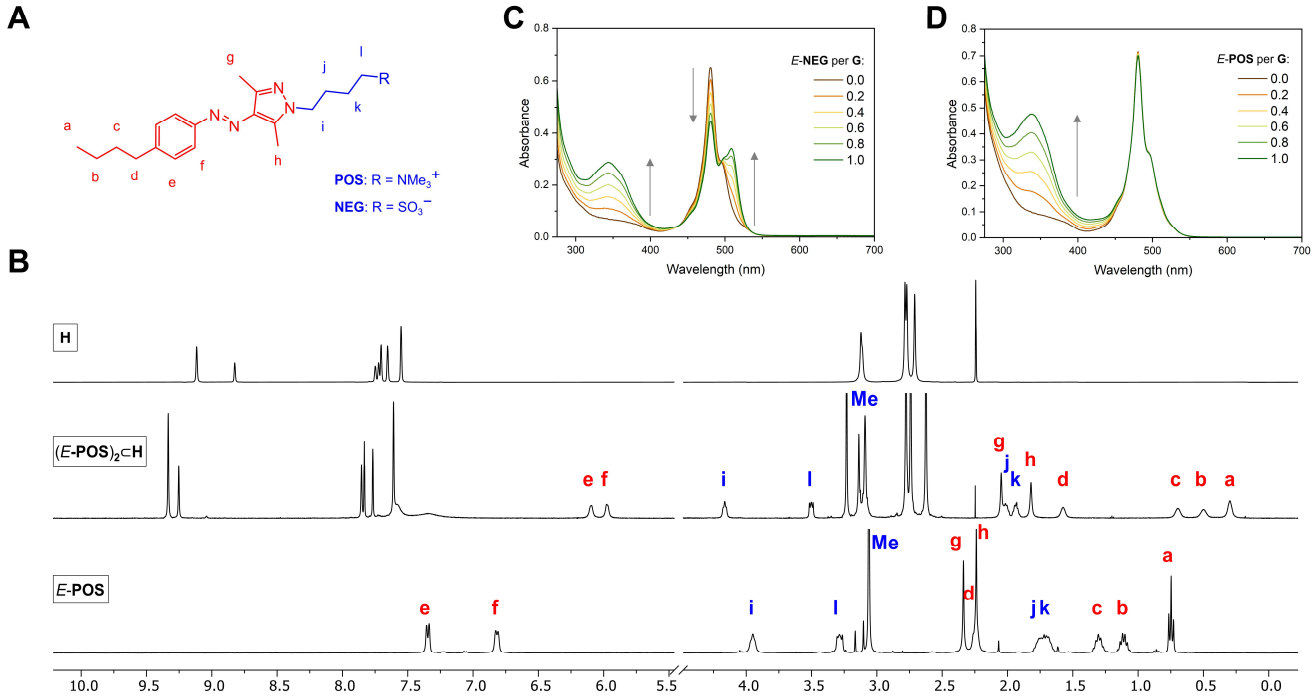

Figure 2. (A) Molecular structure of surfactants **POS** and **NEG**. (B) Top: ^{1}H NMR spectrum of **H** in D_2O (400 MHz, 298 K). Center: ^{1}H NMR spectrum of (*E*-**POS**)$_2$⊂**H** in D_2O (400 MHz, 330 K). Bottom: ^{1}H NMR spectrum of **POS** in D_2O (400 MHz, 298 K). Hydrophobic protons of **POS** (red) experience an upfield shift, while hydrophilic protons (blue) shift downfield. (C) Changes in the UV-vis absorption spectra of an aqueous solution of (**G**)$_2$⊂**H** upon titration with (*E*-**NEG**)$_2$⊂**H**. (D) Changes in the UV-vis absorption spectra of an aqueous solution of (**G**)$_2$⊂**H** upon titration with (*E*-**POS**)$_2$⊂**H**.

ratio of **G** with respect to **NEG** down to 5 mol% extended the reaction time ca. fivefold. Importantly, however, it did not affect the (near-)quantitative formation of *Z*-**NEG**, again proving the process to be significantly quicker than the competing *Z*-to-*E* isomerization induced by the same photon energy (Fig. 3D+E). During these experiments, **H** was present in stoichiometric amounts (one host per two guests). Surfactant disequilibration with green light was also possible using substoichiometric ratios of the host, as aqueous solutions of **NEG** could readily be isomerized to the *E* state upon addition of (**G**)$_2$⊂**H**. For low sensitizer/surfactant ratios (10 mol% and lower), however, we found the photostationary state to contain increasing amounts of *E*-**NEG** due to a deceleration of the reaction kinetics for the sensitized reaction pathway (Fig. S29).

We also studied the DESC mechanism at higher concentrations (4 mM) applying ^{1}H NMR spectroscopy. Under otherwise equal conditions, near-quantitative formation of **NEG**'s *Z* isomer was observed within <5 min of green light irradiation in presence of as little as 2 mol% of **G** (Fig. S30). The resulting NMR spectrum aligned with the spectrum of *Z*-**NEG** within **H** obtained upon direct excitation with UV light in absence of photosensitizer.

Irradiation of (*E*-**POS**)$_2$⊂**H** in presence of **G** analogously resulted in the formation of *Z*-**POS**. ^{1}H NMR spectroscopy showed quantitative formation of the *Z* isomer within <5 min (5 mol% of **G**; Fig. S33). At low micromolar concentration, however, due to the significantly lower probability of **POS** to be associated to **H**, the reaction kinetics were slower by 1-2 orders of magnitude in comparison to **NEG** (Fig. 3F). These slow turnover numbers resulted in a non-quantitative formation of the *Z* isomer due to the increasing impact of the green light-induced direct *Z*-to-*E* isomerization of the surfactant on the resulting photostationary state. This was especially relevant at low photosensitizer loadings, which further decelerated the sensitization pathway.

Surface tension control with green light

To study whether the surface tension of water could be reversibly tuned by visible light using DESC, we turned to tensiometric measurements (see SI chapter 6 for details). Initially, we applied the pendant drop method to study the impact of **H** on the surface activity of the surfactants. We found that the amphiphilic behavior of *E*-**POS** (0.5 mM) was barely affected by the presence of **H**: The surfactant ($c_{E\text{-}\mathbf{POS}}$ = 2.0 mM, $c_{\mathbf{H}}$ = 1.0 mM) still shows a high surface activity (γ = 54.5 mNm^{-1} vs. 53.5 mNm^{-1} for *E*-**POS** only) and is significantly reducing the surface tension of water (Fig. S40A). In a pursuing experiment, we confirmed that an aqueous solution of **H** shows no relevant surface activity (γ = ~72 mNm^{-1}; Fig. S40B).

We continued to apply the pendant drop method (Fig. 4A) in presence of sensitizer **G**. We measured the surface tension of *E*-**POS** under DESC conditions (for all tensiometric measurements, we applied 50 mol% of **H** and 10 mol% of **G**) incl. constant green light irradiation as a function of time. Initially, the pendant drop was formed under ambient conditions and an initial surface tension of 64 mNm^{-1} was detected. Under subsequent irradiation with green light, the

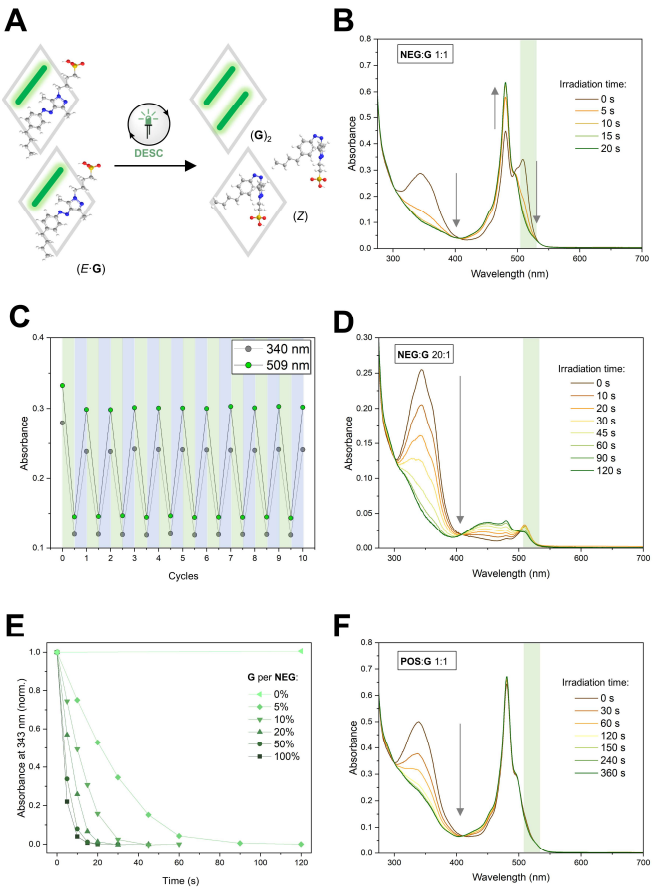

Figure 3. (A) Scheme: Isomerization of **NEG** by DESC. (B) Absorption spectrum of a 1:1 mixture of (**G**)$_2$⊂**H** and (*E*-**NEG**)$_2$⊂**H** and subsequent changes in the spectra accompanying irradiation with 515 nm green light. (C) Ten cycles of photoisomerization of **NEG** by green (515 nm, 30 s) and blue (435 nm, 30 s) light irradiation. The plot follows the absorbance at 340 nm (for *E*-**NEG**) and 509 nm (for (*E*-**NEG**·**G**)⊂**H**). (D) Absorption spectrum of a 1:20 mixture of (**G**)$_2$⊂**H** and (*E*-**NEG**)$_2$⊂**H** and subsequent changes in the spectra accompanying irradiation with 515 nm green light. (E) Graph following the *E*-to-*Z* isomerization of **NEG** enabled by **G** upon 515 nm irradiation in different relative ratios. The absorbance values were normalized from 1 (at t_0) to 0 (PSS), except for the 0% dataset (for which $Abs_0 \approx Abs_{PSS}$). (F) Absorption spectrum of a 1:1 mixture of (**G**)$_2$⊂**H** and (*E*-**POS**)$_2$⊂**H** and subsequent changes in the spectra accompanying irradiation with 515 nm green light.

size of the drop shrank, indicating increasing surface tension, until a plateau was reached at ~71 mNm^{-1}, corresponding to little to no surface activity for **POS** in the resulting photostationary state (Fig. 4B). Including the equilibration time for the changing surface tension, the plateau area (marking the end of the isomerization process) was reached within approximately 150 s, which corresponds well with the time span for the depletion of *E*-**POS** observed in UV-vis experiments discussed above which were conducted under analogous conditions.

Subsequently, an in-depth analysis on the equilibrium surface tension for **POS** under DESC conditions as a function of

its bulk concentration was performed (Fig. 4C). The thermodynamically stable *E* isomer was treated under ambient/dark conditions (black squares), while constant irradiation with 520 nm led to the corresponding photoproduct (green circles). For concentrations lower than 10 mM, the equilibrium surface tension of the air–water interface is systematically lower for **POS** in its *E* state compared to its *Z* configuration. Starting from 7 mM, a plateau in surface tension is observed for the *E* isomer with no significant changes in surface tension beyond this concentration, indicating saturation of the air-water interface with the amphiphile. Hence, no further surface excess change is observed and a process of increased bulk aggregation (micelle formation) can be expected. The difference in surface tension under ambient and dark conditions is attributed to the different surface activity for both **POS** isomers with varying corresponding equilibrium constants for ad- and desorption to and from the air-water interface. As expected, the tensiometric measurements allowed to conclude a higher relative surface activity of the corresponding *E* isomer in comparison to the *Z* state. In agreement with our previous work,[39] the *Z* configuration displays less amphiphilic (and thereby less surface active) behavior than the thermodynamically stable *E* isomer. The change in surface tension (Δγ) under applied conditions upon photoisomerization was measured to be as high as 13 mNm^{-1} (at 7 mM). The presence of host **H** and sensitizer **G** have hence little to no impact on the observed effect of **POS** on water's surface tension in both isomeric states.

To further investigate the visible light responsiveness of the air-water interface and reversibility of the isomerization process induced by DESC, we applied blue light (445 nm) to a pendant drop previously disequilibrated by green light to reverse the reaction and increase **POS**'s surface activity. During four cycles of photoisomerization for **POS** (c = 0.5 mM, chosen due to the relatively large Δγ in combination with a low concentration), a fast increase in the surface tension was observed for the *E*-to-*Z* transition induced by green light, followed by the subsequent, slightly slower decrease in surface tension upon blue light irradiation caused by the transition from the disequilibrated *Z* to the thermodynamically stable *E* state (Fig. 4D). A notable decline of measured surface tension values irrespective of the irradiation is explained by evaporation of water, which is corrected by the instrument but still results in an increasing concentration of the surfactant in the observed drop. Control experiments in absence of sensitizer **G** or host **H** showed no light induced change in the measured surface tension under alternating irradiation with blue (445 nm) and green (520 nm) light (Fig. S38). Equally, irradiating aqueous solutions of **H** or (**G**)$_2$⊂**H** alone did not show analogous effects (Fig. S40B+C).

Surface tension control with red light

To test the generality of our visible light surface tension switching approach, we turned to the red light absorbing phenoxazine-based dye resazurin (**R**). In analogy to the approaches summarized above, heterodimers (*E*-**NEG**·**R**)⊂**H** and (*E*-**POS**·**R**)⊂**H** were prepared by mixing the respective surfactant homodimers with (**R**)$_2$⊂**H**. Analogous to sensitizer **G**, we found only little heterodimer formation with

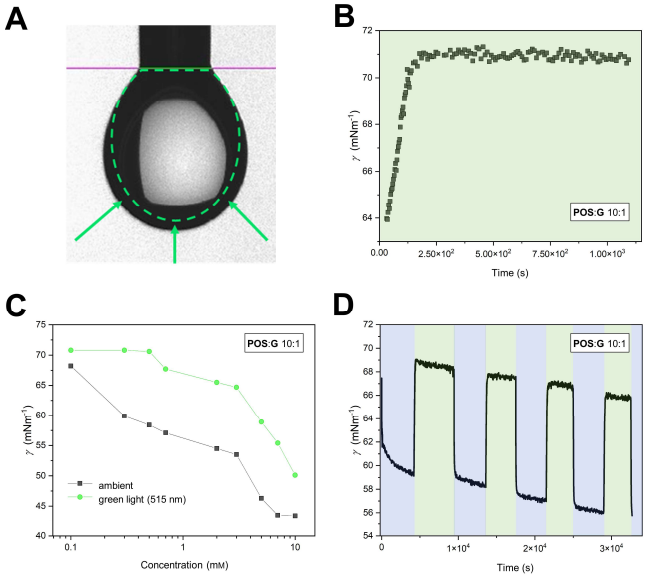

Figure 4. (A) Photograph of the hanging water drop for tensiometric measurements. The green dashed line and arrows schematically illustrate the contraction of the drop due to increased surface tension upon green light sensitized *E*-to-*Z* isomerization of the AAP surfactants. (B) Surface tension measurement of an aqueous solution containing 0.5 mM **POS**, 0.25 mM **H**, and 0.05 mM **G** under green light (515 nm) irradiation. (C) Equilibrium surface tension values of **POS** in the *E* (black squares) and *Z* state (green circles) in dependence of concentration. (D) Four cycles of photoisomerization of **POS** by alternating green (515 nm) and blue (435 nm) light irradiation. The plot follows the surface tension with time. The decline of measured values correlates with the evaporation of water during the experiment.

POS at low concentration (Fig. S25B), while the formation of the *E*-**NEG**·**R** dimer could be followed by the increasing absorption band at ~630 nm (Fig. 5A). Subsequent irradiation of the solutions with red light induced the formation of the surfactant's *Z* isomers. Following the process for **NEG** using UV-vis spectroscopy allowed to observe the parallel decrease of the characteristic *E*-**NEG** and (*E*-**NEG**·**G**)⊂**H** species and the increase of concentration for *Z*-**NEG** and (**R**)$_2$⊂**H** (Fig. 5B). ^{1}H NMR spectroscopy confirmed the successful photoisomerization. The process was reversible using blue light, but the absence of a green light absorbing sensitizer also allowed to steer the back reaction using green (515 nm) light. The ratio of **R** to **NEG** was lowered incrementally to 10 mol%, at which point the reaction was still performing well (Fig. 5C). In view of no back-reaction being induced by red light, further reduction of the sensitizer load was possible but resulted in long equilibration times making the process unattractive for most purposes. These results aligned well with findings by Klajn and co-workers of suboptimal sensitization of AAPs by the red-light absorbing sensitizer **R**, arguably connected with a disadvantageous match of triplet energies.[29] Here, azobenzene-based surfactants are expected to show significantly faster equilibration. Analogous results were found for the sensitized isomerization of **POS**, with again significantly longer equilibration times due to lower levels of formation of the active

heterodimer species (Fig. S36). We pursued tensiometric measurements analyzing to which degree **POS** remains surface active under red light sensitized conditions and investigated dynamic changes at the air-water interface. In view of long equilibration times connected with unfavorable effects on the data quality (especially water evaporation) for low molar ratios of **R** to **POS**, we increased the sensitizer load (for all tensiometric measurements with red light sensitization we applied 50 mol% of **H** and 50 mol% of **R**). The responsiveness of adsorbed **POS** molecules at the air-water interface was investigated in four cycles of photoisomerization for 0.5 mM **POS** applying alternating green and red light (Fig. 5D). Despite the higher catalyst loading, irradiation with red light still resulted in a significantly slower increase in surface tension for *E*-to-*Z* transitions than for the green light sensitized process discussed above. A significant change between both states of $\Delta\gamma \approx 10$ mNm^{-1} could readily be detected. Subsequently, a fast decrease in surface tension upon green light irradiation caused by the transition from the disequilibrated *Z* to the thermodynamically stable *E* state resulted in system equilibration. The solvent evaporation induced decrease of observed surface tension values was analogous to the green light experiment.

CONCLUSIONS

In summary, we studied the implementation of disequilibration by sensitization under confinement (DESC) of AAP-based amphiphiles to modulate the surface tension of water. For a positively (**POS**) and a negatively (**NEG**) charged surfactant, we initially studied binding to host **H** and their ability to form sensitizer·surfactant heterodimers within the macrocycle. Homodimer formation (**POS**)$_2$⊂**H** and (**NEG**)$_2$⊂**H** in aqueous solution was observed, wherein the surfactants retained their light responsiveness, including significant changes in surface tension observed for their *E* or *Z* states, respectively. After formation of heterodimers with green light absorbing BODIPY derivative **G**, both surfactants were reversibly isomerized using green (515 nm) light for the *E*-to-*Z* isomerization and blue light (435 nm) for the reverse process. This sensitized disequilibration was possible both in presence of stoichiometric or sub-stoichiometric amounts of the sensitizer **G** or, with restrictions, host **H**. No fatigue for the sensitizer or surfactant was observed for at least ten cycles of switching under the applied conditions. The tensiometric measurements showed that the difference in surface tension is attributed to the different surface activity of *E*- and *Z*-**POS** while the presence of **H** and **G** have no effect on **POS**'s surface activity while still enabling dynamic changes of the air-water interface by using visible light excitation. Subsequently, we applied the red light (635 nm) absorbing phenoxazine-based dye **R** to enable reversible switching between the inactive/low surface tension state and the active/high surface tension state using red and green light, respectively.

This study marks the first implementation of DESC beyond the small molecule proof-of-concept level. Despite concurrent (e.g., surfactant assemblies and micelle formation) or even counteracting (e.g., green light induced *Z*-to-*E* isomerization of AAPs) processes, the host-sensitizer combination's binding selectivity for *E* amphiphiles enables a (near-)quantitative surfactant disequilibration. In the realm of stimuli-responsive soft matter, the ability to activate multicomponent molecular systems with a selectable wavelength (dependent on sensitizer) promises transformative implications. While demonstrated for assemblies at the air-water interface in the present work, we expect the concept to be equally implementable for other platforms such as hydrogels, solid-water interfaces, or biologically relevant environments.

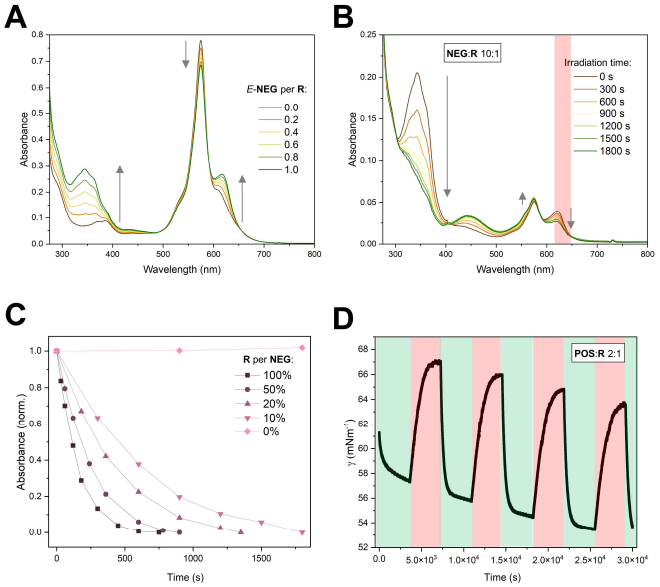

Figure 5. (A) Changes in the UV-vis absorption spectra of an aqueous solution of (**R**)$_2$⊂**H** upon titration with (*E*-**NEG**)$_2$⊂**H**. (B) UV-vis absorption spectrum of a 1:10 mixture of (**R**)$_2$⊂**H** and (*E*-**NEG**)$_2$⊂**H** and subsequent changes in the spectra accompanying irradiation with 635 nm red light. (C) Graph following the *E*-to-*Z* isomerization of **NEG** enabled by **R** upon 635 nm irradiation in different relative ratios. The absorbance values were normalized from 1 (at t_0) to 0 (PSS), except for the 0% **R** data (for which $Abs_0 = Abs_{PSS}$). (D) Four cycles of photoisomerization of **POS** by alternating red (635 nm) and green (520 nm) light irradiation. The plot follows the surface tension with time. The decline of measured values correlates with the evaporation of water during the experiment.

ASSOCIATED CONTENT

Supporting Information

The Supporting Information is available online containing the following chapters:

1. Materials and methods; 2. Synthesis and characterization of host **H** and surfactants **POS** and **NEG**; 3. Synthesis and characterization of homodimeric inclusion complexes; 4. Sensitized isomerization of surfactants in surfactant·photosensitizer heterodimers; 5. Isothermal Titration Calorimetry; 6. Tensiometry; 7. Supplementary references

AUTHOR INFORMATION

Corresponding Authors

Frank Glorius - Organisch-Chemisches Institut, Universität Münster, Corrensstraße 40, 48149 Münster, Germany; Email: glorius@uni-muenster.de

Bart Jan Ravoo - Organisch-Chemisches Institut, Universität Münster, Corrensstraße 40, 48149 Münster, Germany; Email: b.j.ravoo@uni-muenster.de

ACKNOWLEDGMENT

This work was funded by the Deutsche Forschungsgemeinschaft (DFG CRC 1459 Intelligent Matter – Project-ID 433682494).

ABBREVIATIONS

tmeda = tetramethylethylenediamine

REFERENCES

(1) Bandara, H. M. D.; Burdette, S. C. Photoisomerization in different classes of azobenzene. *Chem. Soc. Rev.* **2012**, *41*, 1809–1825.

(2) Jerca, F. A.; Jerca, V. V.; Hoogenboom, R. Advances and opportunities in the exciting world of azobenzenes. *Nat. Rev. Chem.* **2022**, *6*, 51–69.

(3) Mukherjee, A.; Seyfried, M. D.; Ravoo, B. J. Azoheteroarene and Diazocine Molecular Photoswitches: Self-Assembly, Responsive Materials and Photopharmacology. *Angew. Chem., Int. Ed.* **2023**, *62*, e202304437.

(4) Wang, Z.; Erhart, P.; Li, T.; Zhang, Z.-Y.; Sampedro, D.; Hu, Z.; Wegner, H. A.; Brummel, O.; Libuda, J.; Nielsen, M. B.; et al. Storing energy with molecular photoisomers. *Joule* **2021**, *5*, 3116–3136.

(5) Le, M.; Han, G. G. D. Stimuli-Responsive Organic Phase Change Materials: Molecular Designs and Applications in Energy Storage. *Acc. Mater. Res.* **2022**, *3*, 634–643.

(6) Velema, W. A.; Szymanski, W.; Feringa, B. L. Photopharmacology: beyond proof of principle. *J. Am. Chem. Soc.* **2014**, *136*, 2178–2191.

(7) Hüll, K.; Morstein, J.; Trauner, D. In Vivo Photopharmacology. *Chem. Rev.* **2018**, *118*, 10710–10747.

(8) Stoll, R. S.; Hecht, S. Artificial light-gated catalyst systems. *Angew. Chem., Int. Ed.* **2010**, *49*, 5054–5075.

(9) Wei, Y.; Han, S.; Kim, J.; Soh, S.; Grzybowski, B. A. Photoswitchable catalysis mediated by dynamic aggregation of nanoparticles. *J. Am. Chem. Soc.* **2010**, *132*, 11018–11020.

(10) Viehmann, P.; Hecht, S. Design and synthesis of a photoswitchable guanidine catalyst. *Beilstein J. Org. Chem.* **2012**, *8*, 1825–1830.

(11) Osorio-Planes, L.; Rodríguez-Escrich, C.; Pericàs, M. A. Photoswitchable thioureas for the external manipulation of catalytic activity. *Org. Lett.* **2014**, *16*, 1704–1707.

(12) Del Barrio, J.; Horton, P. N.; Lairez, D.; Lloyd, G. O.; Toprakcioglu, C.; Scherman, O. A. Photocontrol over cucurbit[8]uril complexes: stoichiometry and supramolecular polymers. *J. Am. Chem. Soc.* **2013**, *135*, 11760–11763.

(13) Lee, S.; Oh, S.; Lee, J.; Malpani, Y.; Jung, Y.-S.; Kang, B.; Lee, J. Y.; Ozasa, K.; Isoshima, T.; Lee, S. Y.; et al. Stimulus-responsive azobenzene supramolecules: fibers, gels, and hollow spheres. *Langmuir* **2013**, *29*, 5869–5877.

(14) Yagai, S.; Kitamoto, Y.; Datta, S.; Adhikari, B. Supramolecular Polymers Capable of Controlling Their Topology. *Acc. Chem. Res.* **2019**, *52*, 1325–1335.

(15) Fuentes, E.; Gerth, M.; Berrocal, J. A.; Matera, C.; Gorostiza, P.; Voets, I. K.; Pujals, S.; Albertazzi, L. An Azobenzene-Based Single-Component Supramolecular Polymer Responsive to Multiple Stimuli in Water. *J. Am. Chem. Soc.* **2020**, *142*, 10069–10078.

(16) Mukherjee, A.; Ghosh, G. Light-regulated morphology control in supramolecular polymers. *Nanoscale* **2024**, *16*, 2169–2184.

(17) Ahuja, R. C.; Maack, J.; Tachibana, H. Unconstrained Cis-Trans Isomerization of Azobenzene Moieties in Designed Mixed Monolayers at the Air/Water Interface. *J. Phys. Chem.* **1995**, *99*, 9221–9229.

(18) Hou, I. C.-Y.; Diez-Cabanes, V.; Galanti, A.; Valášek, M.; Mayor, M.; Cornil, J.; Narita, A.; Samorì, P.; Müllen, K. Photomodulation of Two-Dimensional Self-Assembly of Azobenzene–Hexa-peri-hexabenzocoronene–Azobenzene Triads. *Chem. Mater.* **2019**, *31*, 6979–6985.

(19) Quintano, V.; Diez-Cabanes, V.; Dell'Elce, S.; Di Mario, L.; Pelli Cresi, S.; Paladini, A.; Beljonne, D.; Liscio, A.; Palermo, V. Measurement of the conformational switching of azobenzenes from the macro- to attomolar scale in self-assembled 2D and 3D nanostructures. *Phys. Chem. Chem. Phys.* **2021**, *23*, 11698–11708.

(20) Klajn, R.; Wesson, P. J.; Bishop, K. J. M.; Grzybowski, B. A. Writing self-erasing images using metastable nanoparticle "inks". *Angew. Chem., Int. Ed.* **2009**, *48*, 7035–7039.

(21) Stricker, L.; Fritz, E.-C.; Peterlechner, M.; Doltsinis, N. L.; Ravoo, B. J. Arylazopyrazoles as Light-Responsive Molecular Switches in Cyclodextrin-Based Supramolecular Systems. *J. Am. Chem. Soc.* **2016**, *138*, 4547–4554.

(22) Hartley, G. S. The Cis-form of Azobenzene. *Nature* **1937**, *140*, 281.

(23) Cembran, A.; Bernardi, F.; Garavelli, M.; Gagliardi, L.; Orlandi, G. On the mechanism of the cis-trans isomerization in the lowest electronic states of azobenzene: S0, S1, and T1. *J. Am. Chem. Soc.* **2004**, *126*, 3234–3243.

(24) Crecca, C. R.; Roitberg, A. E. Theoretical study of the isomerization mechanism of azobenzene and disubstituted azobenzene derivatives. *J. Phys. Chem. A* **2006**, *110*, 8188–8203.

(25) Beharry, A. A.; Sadovski, O.; Woolley, G. A. Azobenzene photoswitching without ultraviolet light. *J. Am. Chem. Soc.* **2011**, *133*, 19684–19687.

(26) Bléger, D.; Schwarz, J.; Brouwer, A. M.; Hecht, S. o-Fluoroazobenzenes as readily synthesized photoswitches offering nearly quantitative two-way isomerization with visible light. *J. Am. Chem. Soc.* **2012**, *134*, 20597–20600.

(27) Yang, Y.; Hughes, R. P.; Aprahamian, I. Visible light switching of a BF_2-coordinated azo compound. *J. Am. Chem. Soc.* **2012**, *134*, 15221–15224.

(28) Gao, M.; Kwaria, D.; Norikane, Y.; Yue, Y. Visible-light-switchable azobenzenes: Molecular design, supramolecular systems, and applications. *Nat. Sci.* **2023**, *3*, e220020.

(29) Gemen, J.; Church, J. R.; Ruoko, T.-P.; Durandin, N.; Białek, M. J.; Weißenfels, M.; Feller, M.; Kazes, M.; Odaybat, M.; Borin, V. A.; et al. Disequilibrating azobenzenes by visible-light sensitization under confinement. *Science* **2023**, *381*, 1357–1363.

(30) Samanta, D.; Mukherjee, S.; Patil, Y. P.; Mukherjee, P. S. Self-assembled Pd_6 open cage with triimidazole walls and the use of its confined nanospace for catalytic Knoevenagel- and Diels-Alder reactions in aqueous medium. *Chem. Eur. J.* **2012**, *18*, 12322–12329.

(31) Isokuortti, J.; Kuntze, K.; Virkki, M.; Ahmed, Z.; Vuorimaa-Laukkanen, E.; Filatov, M. A.; Turshatov, A.; Laaksonen, T.; Priimagi, A.; Durandin, N. A. Expanding excitation wavelengths for azobenzene photoswitching into the near-infrared range via endothermic triplet energy transfer. *Chem. Sci.* **2021**, *12*, 7504–7509.

(32) Bharmoria, P.; Ghasemi, S.; Edhborg, F.; Losantos, R.; Wang, Z.; Mårtensson, A.; Morikawa, M.-A.; Kimizuka, N.; İşci, Ü.; Dumoulin, F.; et al. Far-red triplet sensitized Z-to-E photoswitching of azobenzene in bioplastics. *Chem. Sci.* **2022**, *13*, 11904–11911.

(33) Dutta, S.; Erchinger, J. E.; Strieth-Kalthoff, F.; Kleinmans, R.; Glorius, F. Energy transfer photocatalysis: exciting modes of reactivity. *Chem. Soc. Rev.* **2024**, *53*, 1068–1089.

(34) Samanta, D.; Galaktionova, D.; Gemen, J.; Shimon, L. J. W.; Diskin-Posner, Y.; Avram, L.; Král, P.; Klajn, R. Reversible chromism

of spiropyran in the cavity of a flexible coordination cage. *Nat. Commun.* **2018**, *9*, 641.

(35) Samanta, D.; Gemen, J.; Chu, Z.; Diskin-Posner, Y.; Shimon, L. J. W.; Klajn, R. Reversible photoswitching of encapsulated azobenzenes in water. *Proc. Natl. Acad. Sci. USA* **2018**, *115*, 9379–9384.

(36) Hanopolskyi, A. I.; De, S.; Białek, M. J.; Diskin-Posner, Y.; Avram, L.; Feller, M.; Klajn, R. Reversible switching of arylazopyrazole within a metal-organic cage. *Beilstein J. Org. Chem.* **2019**, *15*, 2398–2407.

(37) Canton, M.; Grommet, A. B.; Pesce, L.; Gemen, J.; Li, S.; Diskin-Posner, Y.; Credi, A.; Pavan, G. M.; Andréasson, J.; Klajn, R. Improving Fatigue Resistance of Dihydropyrene by Encapsulation within a Coordination Cage. *J. Am. Chem. Soc.* **2020**, *142*, 14557–14565.

(38) Schnurbus, M.; Stricker, L.; Ravoo, B. J.; Braunschweig, B. Smart Air-Water Interfaces with Arylazopyrazole Surfactants and Their Role in Photoresponsive Aqueous Foam. *Langmuir* **2018**, *34*, 6028–6035.

(39) Honnigfort, C.; Campbell, R. A.; Droste, J.; Gutfreund, P.; Hansen, M. R.; Ravoo, B. J.; Braunschweig, B. Unexpected monolayer-to-bilayer transition of arylazopyrazole surfactants facilitates superior photo-control of fluid interfaces and colloids. *Chem. Sci.* **2020**, *11*, 2085–2092.

(40) Salonen, A.; Langevin, D.; Perrin, P. Light and temperature bi-responsive emulsion foams. *Soft Matter* **2010**, *6*, 5308.

(41) Chevallier, E.; Monteux, C.; Lequeux, F.; Tribet, C. Photofoams: remote control of foam destabilization by exposure to light using an azobenzene surfactant. *Langmuir* **2012**, *28*, 2308–2312.

(42) Lei, L.; Xie, D.; Song, B.; Jiang, J.; Pei, X.; Cui, Z. Photoresponsive Foams Generated by a Rigid Surfactant Derived from Dehydroabietic Acid. *Langmuir* **2017**, *33*, 7908–7916.

(43) Mamane, A.; Chevallier, E.; Olanier, L.; Lequeux, F.; Monteux, C. Optical control of surface forces and instabilities in foam films using photosurfactants. *Soft Matter* **2017**, *13*, 1299–1305.

(44) Schnurbus, M.; Campbell, R. A.; Droste, J.; Honnigfort, C.; Glikman, D.; Gutfreund, P.; Hansen, M. R.; Braunschweig, B. Photo-Switchable Surfactants for Responsive Air-Water Interfaces: Azo versus Arylazopyrazole Amphiphiles. *J. Phys. Chem. B.* **2020**, *124*, 6913–6923.

(45) Weißenborn, E.; Droste, J.; Hardt, M.; Schlattmann, D.; Tennagen, C.; Honnigfort, C.; Schönhoff, M.; Hansen, M. R.; Braunschweig, B. Light-induced switching of polymer-surfactant interactions enables controlled polymer thermoresponsive behaviour. *Chem. Commun.* **2021**, *57*, 5826–5829.

(46) Hardt, M.; Busse, F.; Raschke, S.; Honnigfort, C.; Carrascosa-Tejedor, J.; Wenk, P.; Gutfreund, P.; Campbell, R. A.; Heuer, A.; Braunschweig, B. Photo-Responsive Control of Adsorption and Structure Formation at the Air-Water Interface with Arylazopyrazoles. *Langmuir* **2023**, *39*, 5861–5871.

(47) Chen, S.; Wang, C.; Yin, Y.; Chen, K. Synthesis of photo-responsive azobenzene molecules with different hydrophobic chain length for controlling foam stability. *RSC Adv.* **2016**, *6*, 60138–60144.

(48) Stricker, L.; Böckmann, M.; Kirse, T. M.; Doltsinis, N. L.; Ravoo, B. J. Arylazopyrazole Photoswitches in Aqueous Solution: Substituent Effects, Photophysical Properties, and Host-Guest Chemistry. *Chem. Eur. J.* **2018**, *24*, 8639–8647.

(49) Weston, C. E.; Richardson, R. D.; Haycock, P. R.; White, A. J. P.; Fuchter, M. J. Arylazopyrazoles: azoheteroarene photoswitches offering quantitative isomerization and long thermal half-lives. *J. Am. Chem. Soc.* **2014**, *136*, 11878–11881.

(50) Mattia, E.; Otto, S. Supramolecular systems chemistry. *Nat. Nanotechnol.* **2015**, *10*, 111–119.

(51) van Esch, J. H.; Klajn, R.; Otto, S. Chemical systems out of equilibrium. *Chem. Soc. Rev.* **2017**, *46*, 5474–5475.

(52) van Rossum, S. A. P.; Tena-Solsona, M.; van Esch, J. H.; Eelkema, R.; Boekhoven, J. Dissipative out-of-equilibrium assembly of man-made supramolecular materials. *Chem. Soc. Rev.* **2017**, *46*, 5519–5535.

(53) Mandal, A. K.; Gangopadhyay, M.; Das, A. Photo-responsive pseudorotaxanes and assemblies. *Chem. Soc. Rev.* **2015**, *44*, 663–676.

(54) Yanshyna, O.; Avram, L.; Shimon, L. J. W.; Klajn, R. Coexistence of 1:1 and 2:1 inclusion complexes of indigo carmine. *Chem. Commun.* **2022**, 58, 3461–3464.

(55) Yanshyna, O.; Białek, M. J.; Chashchikhin, O. V.; Klajn, R. Encapsulation within a coordination cage modulates the reactivity of redox-active dyes. *Commun. Chem.* **2022**, *5*, 44.

(56) Gemen, J.; Białek, M. J.; Kazes, M.; Shimon, L. J. W.; Feller, M.; Semenov, S. N.; Diskin-Posner, Y.; Oron, D.; Klajn, R. Ternary host-guest complexes with rapid exchange kinetics and photoswitchable fluorescence. *Chem* **2022**, *8*, 2362–2379.